Thermal wakes detectability of submerged objects based on scale model

Yang Weiping[1], Zhang Zhilong[1], Li Jicheng[1], Yu Zhong[2]

(1. ATR Laboratory, National University of Defence Technology, Changsha 410073, China;
2. State Key Laboratory of Ocean Engineering, Shanghai Jiaotong University, Shanghai 200240, China)

Abstract: According to similarity principles, an infrared imaging experimental test system was set up based on scale model, several different working conditions in the condition of scale model were designed based vehicle volume, submerged depth, movement, wake discharging, and etc., so that it was possible to realize the static and dynamic thermal wake detection tests of scaled model. The aim is to determine the detectability of thermal wakes from submerged vehicle on one side, and find the influencing factors at thermal wakes detection and changing rules of the wakes to lay a foundation for future work.

Key words: detectability of thermal wakes; scale model; submerged objects; similarity; static test; dynamic test

CLC number: TN219 **Document code:** A **DOI:** 10.3788/IRLA201645.0302002

基于缩比模型的水下目标热尾流可探测性研究

杨卫平[1],张志龙[1],李吉成[1],俞 忠[2]

(1. 国防科学技术大学 ATR 重点实验室,湖南 长沙 410073;
2. 上海交通大学 海洋工程国家重点实验室,上海 200240)

摘 要: 基于相似原理建立了缩比实验测试系统,针对目标大小、潜深、运动、尾流释放等设计了多种不同的工况,可实现缩比模型下热尾流探测的静态和动态测试,一方面确定水下目标热尾流的可探测性,另一方面探索热尾流探测的影响因素和变化规律,为下一步工作奠定基础。

关键词: 热尾流可探测性; 缩比模型; 水下目标; 相似性; 静态测试; 动态测试

收稿日期:2015-07-11; **修订日期**:2015-08-14

基金项目:部委研究项目(7131222);国家自然科学基金(61101185)

作者简介:杨卫平(1968-),教授,博士,主要从事图像智能信息处理、目标识别与跟踪等方面的研究。Email:wpyang@nudt.edu.cn

0 Introduction

Submerged object detection has important roles in civil and military domains. To detect out the latent submerged objects, studying its detective means and methods becomes urgent and important. Now except sonar detection, the detection technique of submerged objects like shoal has several other methods, such as laser radar detection, magnetic detection, and thermal infrared detection, and so on. But each has its limitations and applicable situations. Due to wide observing range, day-and-night working, good disguise, passive work, and other advantages, infrared imaging detection technique was paid more attention. However, on account of the complexity of ocean itself and the limitation of experimental conditions, experimental tests using real objects directly are not only expensive and uncertainty for multiple impact factors, but also hardly to do. In order to explore the laws and detective feasibility of submerged object wakes, the first thing to do is to do indoor emulational experiments. Based on physical scale model, doing systematic experimental tests, searching for detectable boundary conditions and impact factors of wake formation and determining the imaging laws wherein the wake is detectable, have obvious advantages. Therefore, in this paper we designed an infrared imaging experimental test system based on scale model, designed several different working conditions in the condition of scale model based object volume, submerged depth, movement, wake flow emission, and etc, so that it is possible to realize the static and dynamic thermal wake detection tests of scaled objects. The aim is to decide the detectability of thermal wakes from submerged object on one side, and find the impact factors in thermal wakes detection and changing rules of the wakes to lay a foundation for the detection of practical physical submerged objects. Experimental results demonstrate the designed scheme is effective.

1 Similarity theory

In hydrodynamics, one of the two flowing system composed of mechanical similarity is practical flowing phenomenon, called prototype; the other one is reacted flowing phenomenon in the tests, called model. What is called mechanical similarity indicates that various physical variables of the both flowing system have their fixed proportional relationship. For the ordinary flowing motion, mechanical similarity requires the system should have geometric similarity, motion similarity, motivity similarity and other similarities.

It is called geometric similarity when the boundary shape of model is similar to the prototype one. Suppose L_y denotes the length of prototype, L_m denotes the length of model, $\delta_L=L_y/L_m$=constant called model scale. Generally the smaller scale can better reflect the flowing states of the prototype. However, the model scale often can not be made too small because of the limitation of the experimental conditions.

It is called motion similarity when the motion states and trajectory of both flowing phenomenons are similar in geometry or the magnitudes of velocity and acceleration maintain fixed proportional relationship and the orientation is the same. When both of the flowing phenomenons reach motion similarity, the motion trajectory of their corresponding particles is similar in geometry, and their experienced time also has fixed proportion, i.e., the time scale $\delta_t=t_y/t_m$ is constant, at this time the velocity scale $\delta_V=V_y/V_m=\delta_L/\delta_t$ is constant too.

When the magnitudes of various acting forces which act on corresponding points in prototype and model flowing process maintain respectively fixed proportions and the same orientations, it is called motivity similarity. Let F_y and F_m denote the outside force of prototype and model, the force scale δ_F is defined as F_y/F_m. According to the Second Newton′s Law, $F=\rho Wa$, where ρ denotes the density, W denotes the volume, and a denotes the acceleration. Thus $\delta_F=(\rho_y/\rho_m)(W_y/W_m)(a_y/a_m)=\delta_\rho\delta_L^3\delta_a$, where $\delta_a=\delta_L/\delta_t^2$=constant is the acceleration scale, δ_ρ is the density scale. Therefore, the force scale can be expressed as $\delta_F=\delta_\rho\delta_L^2\delta_V^2$.

Newton similarity law is the common law to determine motivity similarity of two fluids. The

outside force F in Newton similarity law is the summation of all the forces acted on the fluid. The primary force acted on the two similarity fluids is gravity. So in the scale model based experimental tests, as long as the gravity satisfies the similarity conditions, the models can reflect the motion states of the fluids. The similarity condition only considering gravity is called gravity similarity rule.

Suppose G_y and G_m are the gravity of prototype and model, respectively, then the gravity scale is $\delta_G=G_y/G_m$. Because $G=\rho Wg$, where g is the gravity acceleration. And then $\delta_G=(\rho_y/\rho_m)(W_y/W_m)(g_y/g_m)=\delta_\rho\delta_L^3\delta_g$.

To guarantee the similarities between model and prototype fluids acted by gravity, they should satisfy the common rules of motivity similarity. Because of only considering the gravity G in act force F, F equals G, that is $\delta_F=\delta_G$. Therefore, $\delta_\rho\delta_L^3\delta_g=\delta_\rho\delta_L^2\delta_V^2$, furthermore, the formula can be reduced as $\delta_V^2/(\delta_L\delta_g)=1$, that is $V_y^2/(g_yL_y)=V_m^2/(g_mL_m)$.

Define

$Fr=V/\sqrt{gL}$, the dimensionless constant Fr stands for the ratio of inertia force and gravity, which is called Froude number, then the gravity similarity rule is $(Fr)_y=(Fr)_m$, that is, the Froude numbers are equal when two fluids with geometry similarity reach motivity similarity and vice versa. Under the condition of the gravity similarity rule, we can obtain correlative scale relations, for example, $\delta_t=\delta_L^{0.5}$, $\delta_V=\delta_L^{0.5}$, and $\delta_F=\delta_L^3$.

For the flow field with geometry similarity, temperature field similarity and thermal flow rate similarity are also needed, that is to say, the temperature of corresponding points is proportionable, and the orientation of thermal flow in the microelement of corresponding points is the same, and the magnitude is proportionable. Suppose θ denotes temperature, q denotes thermal flow, then $\delta_\theta=\theta_y/\theta_m$ is constant, and $\delta_q=q_y/q_m$ is constant, too. In the density-stratified fluid case, for the flow field with geometry similarity, it still requires density field similarity, that is, the density of corresponding points is proportionable, for example, let ρ denote background density, then $\delta_\rho=\rho_y/\rho_m$ is constant.

2 Design of experimental test system of thermal wake detection based on scale model

2.1 Scale model based experimental test system

According to similarity theory, designed the scaled model of one typical submerged object, set up an experimental test system as Fig. 1 so as to do a series of pertinent tests.

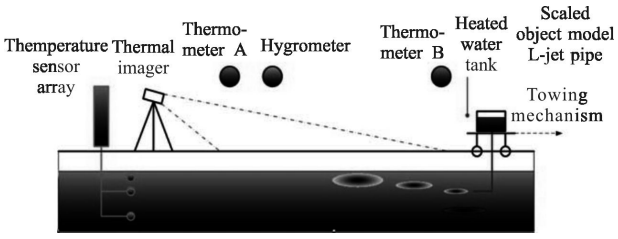

Fig.1 Infrared imaging experimental test system based on scale model

The scale model based infrared imaging experimental test system is composed of eight parts as follows,

(1) Water flume: It owns 30 m in length, 0.6 m in width and 1.2 m in depth. It is employed to simulate the oceanic environment. During the experiment, can add sea salt into fresh water to simulate sea density; prepare stratified seawater by means of twin vats; simulate ocean wave under different state of the sea via fan.

(2) Heated water tank: simulate heat quantity discharged by the object. Change water temperature via heating the water of the tank; change flow velocity via adjusting the height of the tank; change flow rate via adjusting diameter of the L shape jet pipe.

(3) L shape jet pipe: simulate heat quantity discharged by the object. Change flowrate via adjusting diameter of the L shape jet pipe; change submerged depth via adjusting the under-water depth of L shape jet pipe.

(4) Scaled object model: simulate the disturbance caused by the bulk of underwater body and the impact of warm wake buoying process. Precisely control the speed of the scaled model by towing mechanism while

modulate the submerged depth by using bracket.

(5) Towing mechanism: simulate scaled model movement. By means of servo mechanism to control the speed of towing vehicle so as to control the speed of scaled model.

(6) Thermal imager: detect infrared features of thermal wakes in water surface. In the experiment, we will use mid-wave and long-wave cooling thermal imagers.

(7) Thermometers: measure temperatures of atmospheric and water. Where Thermometer A is employed to measure the environment temperature and the water temperature of water flume, Thermometer B is employed to measure the water temperature of the heated water tank, and underwater temperature sensor array is employed to measure the water temperature section plane and water temperature disturbance caused by thermal wake.

(8) Hygrometer: measure the atmospheric humidity.

2.2 Key parameter design of model experiment

Because of the limited depth of water flume, here we adopt the geometry similarity of 1 to 200 to simulate the depth of under-water vehicle. That is to say the water depth in experiment with 0.2 m is equivalent to the practical water depth with 40 m.

Because the motion of thermal jet is mainly buoying, the impact to thermal jet buoying from the bottom of water flume can be ignored. Under the condition of similar Froude number, if thermal buoying is mainly acted by buoyancy, motivity similarity means that the Froude numbers Fr of prototype and model are consistent,

$$Fr=\frac{V}{\sqrt{gL}}$$

The consistent Froude number Fr of density can be expressed as

$$Fr=\frac{V}{\sqrt{gL\dfrac{\Delta\rho}{\rho_a}}}$$

Where ρ_a stands for the surrounding water density, $\Delta\rho$ is the difference of density.

The consistent temperature Froude number Fr can be defined as

$$Fr=\frac{V}{\sqrt{gL\dfrac{\Delta T}{T_a}}}$$

Where T_a stands for the temperature of surrounding water, ΔT stands for the difference of temperature.

According to the above similarities, we can obtain the similarity relationships as follows:

The scale ratio: $L_r=\dfrac{L_p}{L_m}$;

Area ratio: L_r^2;

Volume ratio: L_r^3;

Velocity ratio: $V_r=\sqrt{\dfrac{L_p}{L_m}}$;

Time ratio: $T_r=\dfrac{L_r}{V_r}=\sqrt{L_r}$;

Flowrate ratio: $Q_r=V_r\cdot L_r^2=L_r^{2.5}$.

Referring to the relative parameters of certain object in this paper, we designed the experimental test system according the scale of 1 to 200, then L_r equals 200, the velocity ratio V_r equals 14.1, the time ratio T_r equals 14.1, and the flowrate ratio Q_r equals 565685. Table 1 gives the comparison of main parameters between the practical object and its model.

Tab.1 Parameters of prototype and model with similarity ratio 200

Parameter	Similarity ratio	Practical vehicle	Model
Length	200	107.6 m	0.538 m
Width	200	12.9 m	0.064 5 m
Height	200	10.9 m	0.054 5 m
Under-water depth	200	40 m	0.20 m
		50 m	0.25 m
		60 m	0.30 m
		80 m	0.40 m
		90 m	0.45 m
		100 m	0.50 m
Maximum speed	14.1	25 nod(46.3 km/h)	0.91 m/s
Speed	14.1	5 nod	0.18 m/s
		10 nod	0.36 m/s
Jet pipe diameter	200	0.5 m	2.5 mm
Velocity of draining flow	14.1	1.411 m/s	0.1 m/s
Draining tonnage	565 685	1 000 tons per hour	0.491 047 ml/s

2.3 Working condition design of model tests

Without considering pycnocline, we mainly study the water surface thermal features of moving objects in order to analyze thermal wake detectability of submerged objects. Therefore we designed five working conditions:

(1) Working condition 1: thermal wake detectability tests from static jet flow under different temperatures

Firm the depth of object model and jet flowrate at certain values (e.g. 30 cm for submerged depth, 2.5 mm for jet pipe diameter), change the temperature difference between jet flow water and tank water from 10 centigrade to 65 centigrade and study the detectability of thermal wake from static jet flow under different temperature difference.

(2) Working condition 2: thermal wake detectability tests from static jet flow under different jet flowrate

Firm the depth of object model and jet flow temperature difference values (e.g. 20 cm for submerged depth, 30 centigrade for jet temperature difference), change jet flowrate (according to the scale model, we have designed four jet pipes, the diameters are 2.5 mm, 3.5 mm, 5 mm, 7 mm, respectively. Flowrate changing can be implemented by using different L shape jet pipe diameters) and study the detectability of thermal wake from static jet flow under different jet flowrate.

(3) Working condition 3: thermal wake detectability tests from static jet flow under different depth

Firm jet flow temperature difference and jet flowrate (e.g. 30 centigrade for jet flow temperature difference and 2.5 mm for jet pipe diameter), change the depth from 20 cm to 55 cm and study the detectability of thermal wake from static jet flow under different underwater depth.

(4) Working condition 4: thermal wake detectability tests from towing jet flow under different towing speed

Firm the depth of object model, jet flow temperature difference and jet flowrate (e.g. 20 cm for submerged depth, 30 centigrade for jet flow temperature difference and 2.5 mm for jet pipe diameter), change towing speed (according to the scale model, we have designed two towing speeds, 0.09 m/s and 0.18 m/s) and study the detectability of thermal wake from towing jet flow under different speed.

(5) Working condition 5: thermal wake detectability tests from towing jet flow under different depth

Firm jet flow temperature difference, jet flowrate (e.g. 30 centigrade for jet flow temperature difference and 3.0 mm for jet pipe diameter) and towing speed (0.18 m/s), change underwater depth from 20 cm to 55cm and study the detectability of thermal wake from towing jet flow under different depth.

3 Experimental results and discussion

Based on the above experimental test system and model parameters, we have done more than 100 tests with combined working conditions of different underwater depth, thermal jet flow temperature, water draining time and moving speed, and systematically tested the issues of trajectory of thermal wake buoying, section plane temperature changing, infrared features in water surface and etc. From the five working conditions we can see two kinds of cases are considered, one is the water surface infrared features under the condition of static jet flow in uniform density fluid, the other is the water surface infrared features under the condition of towing jet flow in uniform density fluid.

In order to determine whether or not the wake occurs, we utilize the changes of region gray and region mean deviation with time. The wake occurrence in water surface is cognized when the maximal difference of regional mean gray (absolute gray difference) is larger than 10 or maximal regional gray mean variation difference is larger than 1.5. The larger the absolute difference is, the more obvious the wake is.

The experimental results show that all the tests have good effects no matter what is static jet flow trial or towing jet flow trial in experimental condition. There are obvious thermal wakes in water surface at

the enacted temperature difference, flowrate, under-water depth and moving speed, that is to say, the thermal wake of the submerged object is detectable at the specifically scaled model condition. Table 2 and Table 3 give the test results of thermal wake of the model under the static jet flow and towing jet flow in the uniform density fluid, respectively. The meanings of the data in Tab.3 are equal to those in Tab.2, the values in the table stands for the absolute regional gray difference/regional gray mean variation difference. The experimental results show that the surface thermal wakes are detectable because the absolute regional gray difference is larger than 10 or regional gray mean variation difference is larger than 1.5.

Tab.2 Test results of thermal wake of the vehicle under the static jet flow in uniform density fluid

Scaled water depth/cm	20	35	40	45	50	55				60
Temperature difference ΔT/℃	Pipe diameter 2.5 mm	Pipe diameter 2.5 mm	Pipe diameter 2.5 mm	Pipe diameter 2.5 mm	Pipe diameter 2.5 mm	Pipe diameter 2.5 mm	Pipe diameter 3.5 mm	Pipe diameter 5 mm	Pipe diameter 7 mm	Pipe diameter 2.5 mm
60	–	–	–	–	–	50/5.0	–	––	–	–
55	–	–	–	–	–	50/3.0	–	–	–	–
50	–	–	–	–	–	40/6.0	–	–	–	–
40	–	–	–	–	–	30/5.0	–	–	–	–
30	40/10.0	35/5.0	12/1.5	15/3.0	20/4.5	20/2.5	16/3.0	20/ 2.0	60/10.0	20/2.0
25	–	–	–	–	–	36/5.0	–	–	–	–
20	–	–	–	–	–	15/1.5	–	–	–	–
15	–	–	–	–	–	15/1.5	–	–	–	–
10	–	–	–	–	–	40/5.0	–	–	–	–

Tab.3 Test results of thermal wake of the vehicle under towing jet trial in uniform density fluid

Under-water depth/cm	Speed /m·s^{-1}	Absolute gray difference/Gray mean deviation difference	Detectability	Memo
30	0.18	10/1.5	Obvious	Warm wake
35	0.18	12/1.5	Obvious	Warm wake
40	0.18	15/2.0	Obvious	Warm wake
45	0.18	20/1.5	Obvious	Warm wake
50	0.18	15/1.5	Obvious	Warm wake
55	0.09	15/1.5	Obvious	Warm wake
	0.18	15/1.5	Obvious	Warm wake

Figure 2 gives the typical images of static jet flow experimental tests. Fig.2 (a) gives the mid-wave infrared image and its corresponding long-wave infrared image 14 seconds after the wakes occur, Fig.2 (b) gives the mid-wave infrared image and its corresponding long-wave infrared image 35 s after the wakes occur, where the region marked by red line is the occurrence and changing region of water surface infrared features. Fig.2(c) gives the time varying curves of regional gray mean and gray mean deviation of mid-wave infrared image, which shows that regional gray mean and regional gray mean deviation have obvious fluctuant when the wakes occur. Figure 3 gives the typical infrared images of dynamic towing jet trials. Fig.3 (a) and Fig.3 (b) give the mid-wave infrared images with time interval 39 s. From the figures we can see the image region marked by rectangle has obvious change. Fig.3(c) and Fig.3(d)

give the time varying curves of regional gray mean and gray mean deviation of mid-wave infrared image. From the figures we can see that the gray mean of the image region increases continuously, and the regional gray mean deviation has rolling changes, which shows thermal wakes occur in water surface.

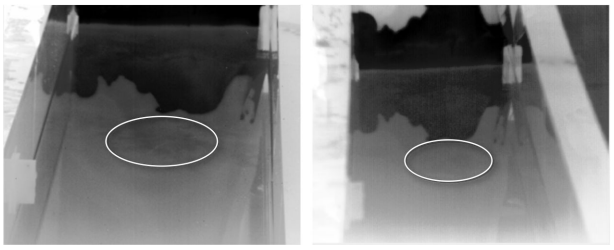

(a) Mid-wave infrared image and its corresponding long-wave infrared image(14 s later) cool wake

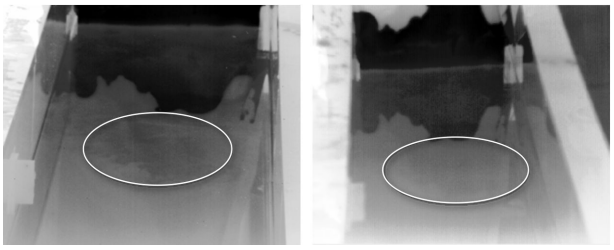

(b) Mid-wave infrared image and its corresponding long-wave infrared image (35 s later) cool wake

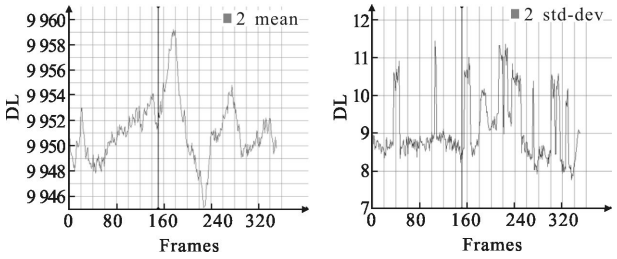

(c) Time varying curves of regional gray mean and gray mean deviation of mid-wave infrared image

Fig.2 Typical image data of static jet trial

(a) Mid-wave infrared image (9 s later)

(b) Mid-wave infrared image (39 s later)

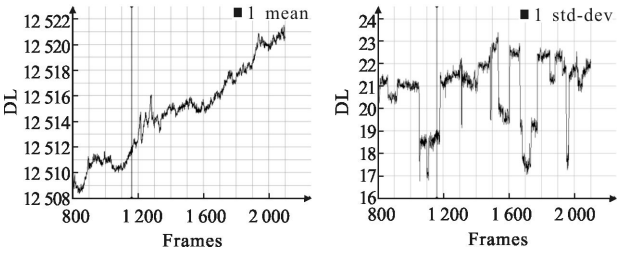

(c) Time varying curve of regional gray mean

(d) Time varying curve of gray mean deviation

Fig.3 Typical image data of towing jet trial(mid-wave infrared image)

Moreover, the design of the scaled model experimental test system can give support for the study of wake buoying features and rules. Limited by the paper, we will discuss it in another paper.

4 Conclusion

Based on similarity theory, set up a scale model based infrared imaging experimental test system for systematic research of wake buoying rules and water surface infrared features. In the experiment, we designed five working conditions under the cases of static jet flow and towing jet flow. On this condition we deeply studied the detectability of thermal wakes by using scaled model in experimental environment and found that thermal wake of scaled object model is detectable which provides experiences for further study of thermal wakes detection. However, because the factors of atmospheric environment temperature, water temperature of the flume, air humidity and the working condition of thermal imager have great impact on the detectability of thermal wakes, the experiment study needs to be deepened. Additionally the practical ocean environment is more complicated, so there is a long way to go for the detection of thermal wakes of submerged object.

References:

[1] Sanjaya Kumar Swain, Trinath K, Tatavarti. Non-acoustic detection of moving submerged Bodies In ocean [J]. ***International Journal of Innovative Research and Development***, 2012, 1(10): 361-372.

[2] Wren G G, May D. Detection of submerged vessels using remote sensing techniques [J]. ***Australian Defence Force Journal***, 1997, 127: 9-15.

[3] Nan Zou, Arye Nehorai. Detection of ship wakes using an airborne magnetic transducer [C]//Proceedings of the 1998 32nd Asilomar Conference on Signals Systems & Computers, 1998, 2: 1316-1321.

[4] Tomokazu Kawahara, Shiyunichi Todaz, Akio Mikamiz, et al. Automatic ship recognition robust against aspect angle changes and occlusions [C]//2012 IEEE Radar Conference (RadarCon), 2012: 864-873.

[5] Feba D Benny, Sanjaya Kumar Swain, Trinath K, et al. System for monitoring underwater turbulence[C]//Proceedings of National Conference on Advanced Communication and Computer Technologies (ACCT), 2012: 381-385.

[6] Zhao Changming, Huang Jie. Development of laser-submarine communication and detection technology in the future [J]. ***Optical Technique***, 2001, 27(1): 53-56. (in Chinese)

[7] Ma Zhiguo, Wang Jiangan. A new method for detecting submarine by laser [J]. ***Journal of Naval University of Engineering***, 2002, 14(6): 77-79, 83. (in Chinese)

[8] Cui Guoheng, Yu Dexin. Status quo of non-acoustics antisubmarine detecting technology and its countermeasures [J]. ***Fire Control and Command Control***, 2007, 32 (12): 10-13. (in Chinese)

[9] Wang Zudian. Airborne anti-submarine non-acoustic detection equipment [J]. ***Electronics Optics & Control***, 2006, 13 (4): 6-9. (in Chinese)

[10] Wan Jun, Zhang Xiaohui, Rao Jionghui, et al. Processing of backscattering signal of warship wake flow based on independent component analysis [J]. ***Infrared and Laser Engineering***, 2013, 42(1): 244-250. (in Chinese)

[11] Lu Xinping, Shen Zhenkang. Analysis of IR imaging system used in anti-submarine detection [J]. ***Infrared and Laser Engineering***, 2002, 31(3): 217-220. (in Chinese)

[12] Jiang Chuanfu, Yang Kuntao, Wang jiang′an, et al. Detection of submarines by air borne IR imaging system [J]. ***Journal Huazhong Univ of Sci & Tech*** (***Nature Science Edition***), 2006, 34(7): 90-92. (in Chinese)

[13] Wang Jiang′an, Guo Yan, Gu Jiannong. The theoretical and trial study of thermal wake in the infrared detection of submarines[J]. ***Laser & Infrared***, 2002, 32(3): 159-162. (in Chinese)

[14] Wu Mengmeng, Chen Boyi, Yang Li. The study progress and application on the surface features of wake behind a going body underwater [J]. ***Infrared Technology***, 2009, 31 (11): 639-646. (in Chinese)